

Article

The Research of Multi-Node Collaborative Compound Jamming Recognition Algorithm Based on Model-Agnostic Meta-Learning and Time-Frequency Analysis

Qing Zhao ¹, Sicun Han ², Wenhao Chen ^{3,4}, Jing He ⁵ and Chengjun Guo ^{6,*} 

¹ Research Institute of Electronic Science and Technology, University of Electronic Science and Technology of China, Chengdu 611731, China; 202121230138@std.uestc.edu.cn

² Rensselaer Polytechnic Institute Troy, New York, NY 12180, USA; hans9@rpi.edu

³ Southwest China Institute of Electronic Technology, Chengdu 610036, China; chenwenhao3@cetc.com.cn

⁴ National Key Laboratory of Complex Aviation System Simulation, Chengdu 610063, China

⁵ Power China Sichuan Electronic Power Engineering Co., Ltd., Chengdu 610056, China; hejing-sedc@powerchina.cn

⁶ School of Automation Engineering, University of Electronic Science and Technology of China, Chengdu 611731, China

* Correspondence: johnsonguo@uestc.edu.cn

Abstract: Deep learning has presented its spectacular potential in the jamming recognition field. Yet, sufficient samples required by normal deep learning analysis methods are not always available, especially in the 6G communication field. This situation appears to be more challenging in the communication field. In this article, Model-Agnostic Meta-Learning (MAML) is imported into the jamming recognition field in order to accomplish compound jamming recognition in the circumstances of few-shot learning. Further, the existing research on jamming recognition techniques is mostly based on single-node recognition. This technique cannot make full and efficient use of the jamming information collected. Therefore, this article adds a multi-node collaborative technique into the compound jamming recognition algorithm that is based on MAML and time-frequency analysis. Based on the fact that each cognitive node can recognize independently, the recognition results are be sent to the fusion center. The fusion center completes the fusion of the recognition results according to the majority rule. The experiments demonstrate that, with the fusion of the multi-node collaborative technique, the precision of compound jamming recognition in the condition of few-shot learning has been effectively improved.

Keywords: jamming recognition; Model-Agnostic Meta-Learning (MAML); few-show learning; multi-node collaboration; 6G



Citation: Zhao, Q.; Han, S.; Chen, W.; He, J.; Guo, C. The Research of Multi-Node Collaborative Compound Jamming Recognition Algorithm Based on Model-Agnostic Meta-Learning and Time-Frequency Analysis. *Electronics* **2024**, *13*, 2772. <https://doi.org/10.3390/electronics13142772>

Academic Editor: Sotirios K. Goudos

Received: 11 June 2024

Revised: 2 July 2024

Accepted: 10 July 2024

Published: 15 July 2024



Copyright: © 2024 by the authors. Licensee MDPI, Basel, Switzerland. This article is an open access article distributed under the terms and conditions of the Creative Commons Attribution (CC BY) license (<https://creativecommons.org/licenses/by/4.0/>).

1. Introduction

In the 6G communication field, the 6G network is able to realize the integration of cellular positioning and communication [1]. And the reliability of 6G communication systems is extremely important for these features. Yet, with the development of radio jamming technology, the 6G communication system is facing a more difficult challenge [2]. For example, in [3], the authors could destroy the availability of spectrum resources through radio jamming and then disrupt the packet transmission in 6G communication. Also, in [4], the authors proved a method that could interfere with the users' equipment and reduce the positioning accuracy by transmitting jamming signals. Jamming recognition technology could help the communication system to better cope with various electromagnetic jamming, strengthen the anti-jamming ability of the communication system, and maintain stability even in a harsh environment [5]. According to different classification methods, jamming recognition algorithms can be divided into traditional jamming recognition algorithms and deep-learning-based jamming recognition algorithms.

The traditional jamming recognition algorithm works mainly through the extraction of jamming features, and then completes the jamming signal recognition through machine learning and other methods [6]. The extracted jamming features could be time-domain features, such as time-domain kurtosis, time-domain peak-to-average ratio, and time-domain compression gain; frequency-domain features, such as frequency-domain peak-to-average ratio, spectrum flatness index, and frequency-domain kurtosis; or transform-domain features, such as time–frequency line slope, compression gain, and waveform fractal dimension. The work in [7] proposed a jamming recognition algorithm based on Support Vector Machine (SVM). The algorithm extracted the moment coefficient of kurtosis in the frequency domain and the skewness of four kinds of jamming signals, and then sent the two coefficients to the SVM recognition model to complete the recognition of the jamming signals. In [8], genetic algorithm (GA) was used to optimize SVM classifiers. A GA-SVM was proposed which helped the jamming recognition rate reach 93.34%. The work in [9] established a mixed entropy dataset by extracting four different entropy features of three kinds of GPS jamming signals, and then used Random Forest (RF) to complete the classification and recognition of datasets. The experimental results proved that RF could guarantee the recognition rate of all three kinds of GPS jamming signals. In conclusion, even though the traditional jamming recognition algorithms have the advantage of low complexity, they still need users to manually extract jamming features. In addition, the feature compression of jamming signals is large. Such feature compression will lead to the loss of information, resulting in low accuracy of jamming recognition.

In recent years, deep learning has played an extremely important role in the field of jamming recognition. Through convolutional neural network (CNN), the features of various jamming signals can be automatically extracted to complete the classification task. As shown in Figure 1, according to the difference of the extracted jamming features, jamming recognition algorithms based on deep learning could be divided into four categories: algorithms based on time-domain feature extraction; algorithms based on frequency-domain feature extraction; algorithms based on time–frequency-domain feature extraction; and algorithms based on joint-domain feature extraction. The jamming recognition algorithm based on time-domain feature extraction takes the time-domain sequence of the jamming signal as the algorithm input, and then processes the signal in the time domain, combining the original I path and the Q path, as well as the phase and the amplitude. The work in [10] designed two one-dimensional convolutional neural networks, and took the collected time-domain I/Q data as the input of the two neural networks. The authors fused the output of the two networks. A good jamming classification effect was captured. In [11], the authors combined the phase and the amplitude of the ISM band wireless jamming signal, and used them as the input of the neural network, obtaining a good classification effect. The jamming recognition algorithm based on frequency-domain feature extraction mainly takes the frequency domain sequence of the jamming signal as the input of the neural network. A Wireless Interference Recognition Transformer (WIR-Transformer) network was proposed in [12]. The authors introduced regional division; self-attention was independently calculated. This ensured the accuracy of jamming recognition, and reduced the complexity effectively at the same time. Then, the frequency-domain sequence is taken as the input of the network to complete the classification of 13 kinds of jamming signals. The jamming recognition algorithm based on transform-domain feature extraction takes the time–frequency-domain feature as the input of the neural network. The time–frequency-domain feature can reflect both the time-domain feature and the frequency-domain feature of the jamming signal, and also the characteristics of the jamming signal in multiple dimensions. The work in [13] used the jamming signal time–frequency image obtained by short-time Fourier transform as the input of the VGGNet-16 network and achieved recognition of six kinds of jamming signals under low-JNR conditions. The jamming recognition algorithm based on joint-domain feature extraction takes multiple jamming features as the input of the neural network. The work in [12] combined information of the time–frequency domain and frequency domain, and applied it to the MDN-TFI network and MDN-FS network, respectively, in order to

extract the features of jamming signals. At the same time, three fusion mechanisms of CT, PT, and CA have been proposed for further improving the recognition accuracy of jamming signals. The jamming recognition algorithms mentioned above are all great but studied only in the case of a large number of samples. We considered the situation, that in reality, a large number of jamming samples is not always available. In addition, multiple nodes exist in 6G communication systems. But current jamming recognition algorithms are mostly studied on the basis of a single node. Jamming information from multiple nodes cannot be used effectively. Therefore, how to make full use of the jamming information from multiple nodes is also a very important question to be considered for the accuracy.

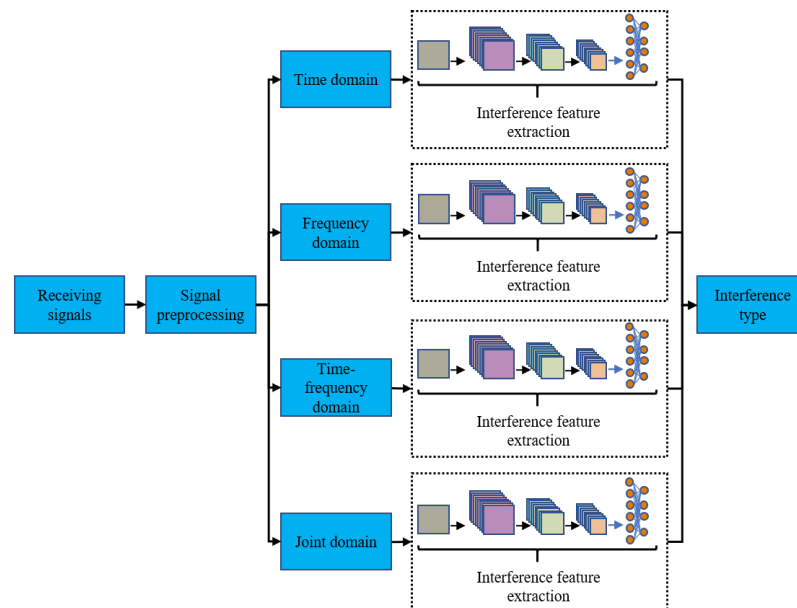


Figure 1. Four jamming recognition algorithms based on deep learning.

In this article, we proposed a multi-node collaborative jamming recognition algorithm based on MAML and time–frequency analysis. The most significant contributions that we have made in this article are as follows:

- (1). We introduced the MAML algorithm into the jamming recognition process, simulated a variety of single jamming signals as a training set, and gained a set of parameters through training, which can realize the recognition of compound jamming signals when the data amount of compound jamming signals is limited.
- (2). We used the Omniglot dataset in order to complete the expansion of the jamming signal dataset, which would make the recognition network have better scalability and generalization, therefore improving the recognition accuracy of the complex jamming signal.
- (3). We introduced the multi-node collaboration idea into few-shot learning compound jamming recognition. Multiple jamming recognition nodes were set up, and each individual node could complete the jamming recognition task independently. The jamming recognition results would be sent to the jamming information fusion center, and the final recognition results would then be obtained by combining the jamming recognition results of multiple nodes. This effectively improved the jamming recognition accuracy.

2. Signal Model and Pre-Processing

2.1. Signal Model

The signal model received by the signal receiver could be expressed as [10]

$$r(t) = J(t) + n(t) \quad (1)$$

where $r(t)$ represents the signal that the signal receiver received, $J(t)$ represents the jamming signal, $n(t)$ represents the white Gaussian noise (WGN).

The single jamming signals used in this article include Single Tone Jamming (STJ), Multi-Tone Jamming (MTJ), Partial Band Noise Jamming (PBNJ), Pulse Jamming (Pulse Jamming) Comb Spectrum Noise Jamming (CSNJ), Linear Frequency Modulation Jamming (LFMJ), Noise Frequency Modulation Jamming (NFMJ), and Sinusoidal Frequency Modulation Jamming (SFMJ). The compound jamming signal studied in this article is obtained by combining STJ, MTJ, PJ, and LFMJ. A total of four kinds of compound jamming signals, STJ-PJ, STJ-LFMJ, STJ-SFMJ, and MTJ-PJ, can be obtained through combination.

2.2. Signal Pre-Processing

For the neural network to better capture the time-domain and frequency-domain features of the signals, the time–frequency image is used as the input of the convolutional neural network [14]. After obtaining the time-domain signal, the time–frequency image of the received signal could be produced by applying short-time Fourier transform to the signal. The formula of short-time Fourier transform is [15]:

$$\text{STFT}[m, k] = \sum_{n=0}^{N-1} r[n]w^*[n - mL]e^{-j\frac{2\pi kn}{N}} \quad (2)$$

where m represents the discrete index of time, k represents the discrete index of frequency, $r[n]$ represents the received time-domain signal, $w[n]$ represents the window function, L represents the length of a time-domain signal, and N represents FFT points.

By functioning short-time Fourier transform, we obtained eight kinds of single jamming signals and four kinds of compound jamming signals. According to the time–frequency uncertainty principle, the time resolution and frequency resolution of the spectrum are mutually restricted when the time–frequency analysis window area is certain. The highest accuracy cannot be achieved at the same time. In addition, different types of jamming signals have different requirements for resolution. Therefore, it is necessary to balance the needs of different jamming signals when selecting the window length. At the same time, there needs to be a certain overlap ratio between adjacent time windows to ensure that the time–frequency curve of non-stationary jamming becomes smooth and avoids obvious distortion [16]. As shown in Figures 2 and 3, different types of jamming signals can be clearly classified by time–frequency characteristics; similarly, other jamming in the real world can be classified by time–frequency characteristics as well.

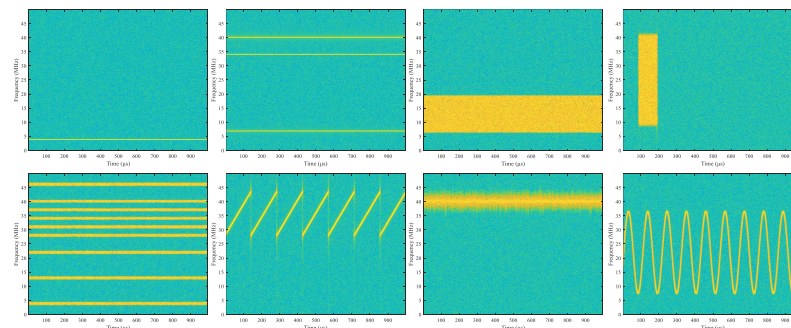


Figure 2. Time–frequency diagram of eight single jamming signals.

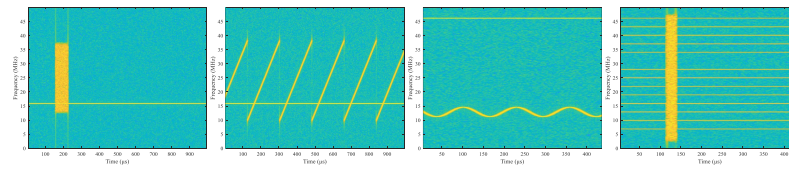


Figure 3. Time–frequency diagram of four compound jamming signals.

3. Multi-Node Collaborative Compound Jamming Recognition Based on Time–Frequency Graph and MAML

3.1. Basic Principles of MAML

Model-Agnostic Meta-Learning (MAML) is an optimization-based algorithm [17]. It can update model parameters iteratively through related tasks so that the training model can quickly adapt to new tasks. The MAML dataset includes a training set and test set; the training set and test set can be divided into the support set and query set. The dataset categories and corresponding functions in the MAML algorithm are shown in Figure 4.

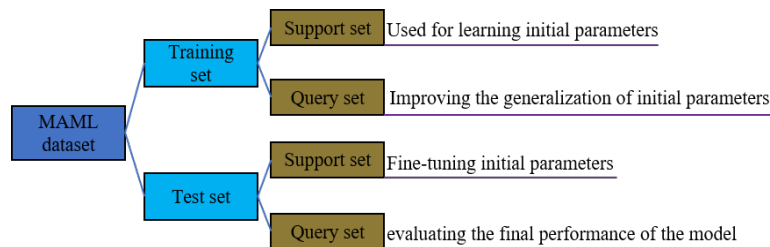


Figure 4. MAML datasets and corresponding functions.

The core idea of MAML is to train a set of highly generalized initialization parameters, so that only a small amount of data would be required to complete one or more steps of gradient adjustment for a new task. As shown in Figure 5, the objective of MAML is to find a set of initialization model parameters θ that is sensitive to task changes; consequently, when the parameters start to change along with the gradient of the loss function \mathcal{L} , a parameter $\bar{\theta}$ that is also sensitive to new tasks will be generated.

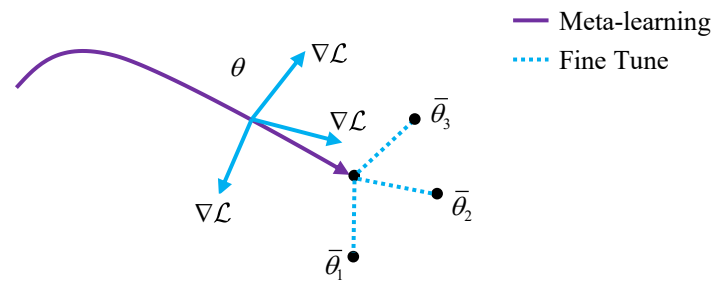


Figure 5. Diagram of MAML adapting to a new task.

As shown in Figure 6, there are two parameter update processes in MAML, namely two gradient descent processes. One is the parameter update that takes place during each task. The other is the parameter update after each set of tasks is completed.

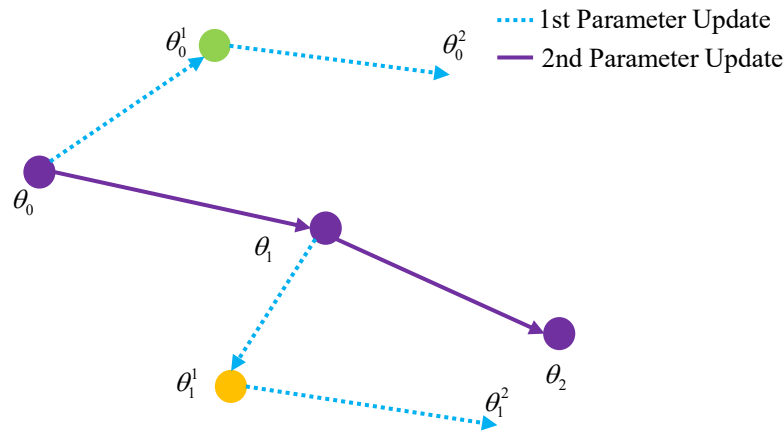


Figure 6. Two kinds of MAML parameter update processes.

Assuming that the task set T_X has a total of S_n group tasks, for the y th task of the group v task, its update formula is as follows:

$$\hat{\theta}_v^y = \theta_v^y - \alpha \nabla_{\theta_v^y} \mathcal{L}^y(f_{\theta_v^y}) \tag{3}$$

where α represents the learning rate of the first gradient descent. When the group v task training is completed, the second parameter update will be carried out. Its update formula is as follows:

$$\theta_{v+1} = \theta_v - \lambda \nabla_{\theta_v} \mathcal{L}(f_{\theta_v}) \tag{4}$$

$$\mathcal{L}(f_{\theta_v}) = \sum_{y=1}^{S_v} \mathcal{L}^y(f_{\hat{\theta}_v^y}) \tag{5}$$

where λ represents the learning rate of the second gradient descent, and S_v represents the total number of tasks in the v th sample group.

3.2. Compound Jamming Recognition Based on Time–Frequency Image and MAML

This article used the MAML algorithm to complete the recognition of compound jamming signals; the diagram is shown in Figure 7. First, we used single jamming to train the network parameters. Single jamming includes Single Tone Jamming (STJ), Multi-Tone Jamming (MTJ), Partial Band Noise Jamming (PBNJ), Pulse Jamming (PJ), Comb Spectrum Noise Jamming (CSNJ), Linear Frequency Modulation Jamming (LFMJ), Noise Frequency Modulation Jamming (NFMJ), and Sinusoidal Frequency Modulation Jamming (SFMJ). Four types of jamming were combined into the tasks each time. Use these tasks as the sample to train the network parameter θ . Predict the support set of the v th and y th tasks through the network, and obtain loss function $\mathcal{L}^y(f_{\theta_v^y})$. Upgrade parameters as function (3), and apply the upgraded network parameter $\hat{\theta}_v^y$ to the search set of the v th and y th tasks. Obtain loss function $\mathcal{L}(f_{\theta_v})$ on task y . Finally, according to function (5), obtain the v th jamming signal task loss function $\mathcal{L}(f_{\theta_v})$, and complete the upgrade of the MAML parameter according to function (4).

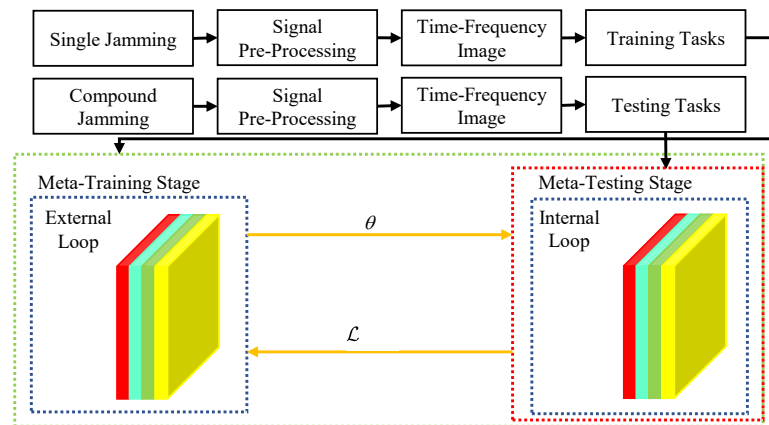


Figure 7. Diagram of MAML compound jamming recognition.

Figure 8 shows the initial network parameter update diagram of the compound recognition algorithm based on MAML. The network parameters obtained after meta-training are then used to initialize the network, and the support set and query set of the new task are composed of four kinds of compound signals to be classified, including STJ-PJ, STJ-LFMJ, MTJ-PJ, and MTJ-LFMJ. Finally, fine-tune the network parameters with the support set in the new task.

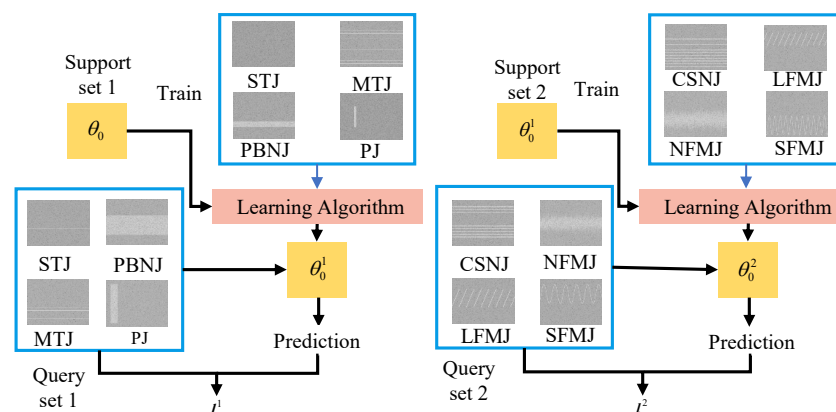


Figure 8. Initial network parameter update diagram of the compound jamming recognition algorithm based on time–frequency image and MAML.

3.3. Multi-Node Collaborative Compound Jamming Recognition Algorithm Based on MAML and Time–Frequency Analysis

6G communication normally involves multiple nodes. These nodes can be land units, sea units, or air units. Through 6G communication, information is transferred and shared between these nodes. Similarly, the nodes in the 6G communication field can be used to collect the jamming signals as well. Based on this, we integrated the idea of multi-node collaboration [18–20] into the compound jamming recognition in the condition of few-shot learning, and proposed a multi-node collaborative compound jamming recognition algorithm based on the time–frequency image and MAML. As shown in Figure 9, the trained and fine-tuned MAML model will be distributed to each communication node. Each cognitive node has the capability of collecting jamming signals and recognizing compound jamming signals through the MAML method independently. After this, the compound jamming recognition results will be sent to the fusion center. The fusion center fuses the jamming recognition results from each node, and produces the final jamming recognition result. The specific flow of Algorithm 1 is shown in the following table.

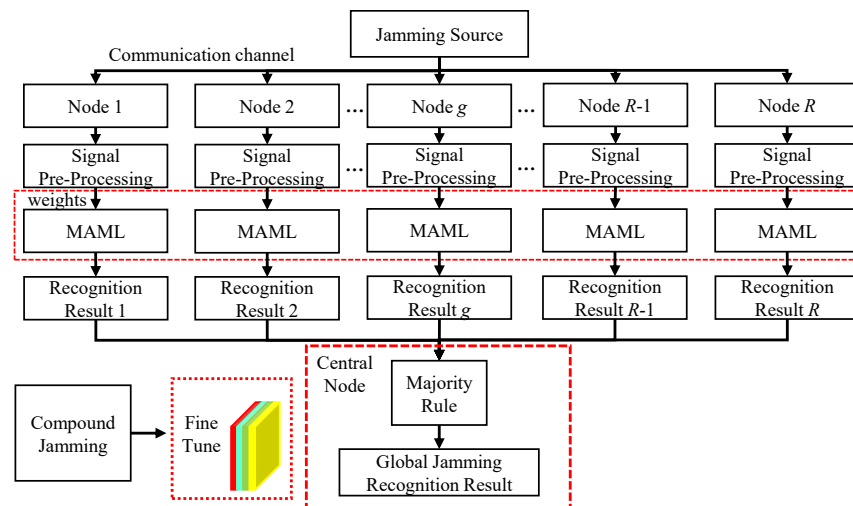


Figure 9. Diagram of multi-node collaborative compound jamming recognition algorithm based on MAML and time–frequency analysis.

Algorithm 1: Multi-node collaborative compound jamming recognition algorithm based on MAML and time–frequency image

Input: Signals received by multi-nodes

Output: Global compound jamming recognition results

1. Use eight different kinds of single jamming signals to train the MAML network parameters and deploy the network parameters to each node.
 2. Each node collects jamming signals, respectively.
 3. Each node completes pre-processing of jamming signals, transforming the signals from one-dimensional sequence to time–frequency images.
 4. Each node completes recognition of compound jamming signals through MAML algorithm independently.
 5. Each node sends jamming recognition results to the central node. Central node completes the fusion of jamming recognition results from multi-nodes based on majority rule and finally produces the final recognition result.
-

4. Analysis of the Simulation and Experimental Results

4.1. Experimental Parameter Setting and Dataset Description

In the process of the simulation experiment, the compound jamming signal and the time–frequency image dataset were generated on the Matlab R2019b platform. The MAML algorithm was implemented using PyTorch 1.13.1 on the PyCharm 2020.1 × 64 platform. In the process of short-time Fourier transform toward one-dimensional time-domain sequence, we set the time-domain segment length to be 512 sampling points and the overlap length between adjacent Windows to be 440 sampling points.

For the eight kinds of single jamming used for meta-training nodes, we generated 100 sets of signals under each JNR at 2 dB intervals as the meta-training datasets. In order to better conform to the real communication environment, the settings for generating single tone jamming are shown in Table 1.

For four kinds of compound jamming signals to be classified, we generated 200 groups of signals under each JNR at 2 dB intervals as the test set. Then, we extracted 32 sets of data from each class as the support set for the test set, which is used to fine-tune the network parameters to achieve the four-way 32-shot classification task. After that, we extracted 100 groups of data from each class under each JNR as the query set of the test set (the query set and the support set are not repeated) for testing the classification performance. Each group of the query set contains 21 time–frequency images generated by adding noise to the same jamming signal, which were used to simulate the compound jamming signal received

by multiple nodes. The parameter setting of the compound jamming signal is shown in Table 2. W_r represents the power ratio of two single jamming signals in the composite jamming signal; the value range is from 0.8 to 1.2. The purpose is to avoid a single jamming signal component significantly suppressing another. F_b represents the band relationship between two single jamming signals in a composite jamming signal, and its value is \emptyset . This is also for avoiding a single jamming signal component significantly suppressing another. Finally, we set the learning rate of the inner loop to 0.05, the learning rate of the outer loop to 0.001, and the training epoch to 10,000.

Table 1. Parameter setting of eight single jamming signals.

Signal Type	Bandwidth Range	Parameters Setting
Sampling Frequency f_s	—	50 MHz
Single Tone Jamming	—	Random Carrier Frequency
Multi-Tone Jamming	—	Random Tone Amounts: 3–15
Partial Band Noise Jamming	0.03~0.8	—
Pulse Jamming	0.04~0.98	Duration Time: 20 μ s~120 μ s
Comb Spectrum Noise	—	Random Tone Amounts: 3–15
Linear Frequency Modulation Jamming	0.04~0.8	—
Noise Frequency Modulation Jamming	0.02~0.2	—
Sinusoidal Frequency Modulation Jamming	0.04~0.8	—

Table 2. Parameter setting of four compound jamming signals.

Parameter Type	Parameter Setting
W_r	0.8~1.2
F_b	\emptyset

In the MAML training process, the amount of samples of each type is very limited. In order to make the network suitable for various types of tasks, more types of tasks would be required for the training process. However, since the category of single jamming signals used for training in this article is also very limited, expanding the dataset is a necessary operation. The Omniglot dataset is a classic few-shot learning dataset, which includes 1623 handwritten characters in 50 different languages, with 20 samples for each character [21]. As shown in Figure 10, character recognition is also realized through the characteristics of lines, which is similar to the time–frequency diagram of compound jamming. Therefore, extending the dataset in this article with the Omniglot dataset is valid.

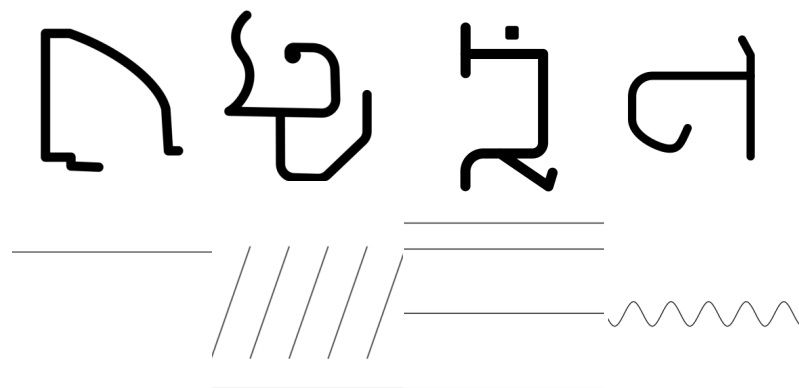


Figure 10. Comparison of the compacted jamming signal with the Omniglot dataset.

4.2. Compound Jamming Recognition Performance Based on MAML and Time–Frequency Analysis

In this section, we will demonstrate the results of compound jamming recognition based on MAML. The network used in this article is Resnet18. First, we trained the MAML network using eight kinds of single jamming signals and set up 8000 epochs to complete the training process. Then, on the basis of four kinds of compound jamming, we completed the fine-tuning of the MAML network. Finally, we tested the recognition accuracy of the MAML network on four kinds of complex jamming.

As shown in Figure 11, by observing the overall recognition accuracy curve of the compound jamming recognition algorithm based on MAML in this article, we cannot but notice that compared with the model using a single jamming signal and the Omniglot dataset, the model using only eight single jamming signals does not have an ideal recognition effect on the compound jamming signal. This is because there are too few types of tasks in the meta-training stage. The lack of task diversity in the meta-training results in the poor generalization ability of the model on new tasks. With the increase in JNR, the overall recognition accuracy of the compound jamming presented an increasing trend. Under the conditions of high JNR, the overall recognition accuracy was close to 100%, which guaranteed the effectiveness of the proposed algorithm. At the same time, the recognition accuracy of four kinds of compound jamming signals is shown in the figure. With the improvement of JNR, the recognition accuracy of each type of compound jamming signal shows an increasing trend. When $JNR = -8$ dB, the recognition accuracy of each type of compound jamming reached 90%. After $JNR = 0$ dB, the recognition accuracy of the four compound jamming signals was close to 100%, which further ensured the performance of the compound jamming recognition algorithm based on MAML. In this article, we counted the number of parameters and Flops of the network, in which Params is 11.7 M and Flops is 1.82 G.

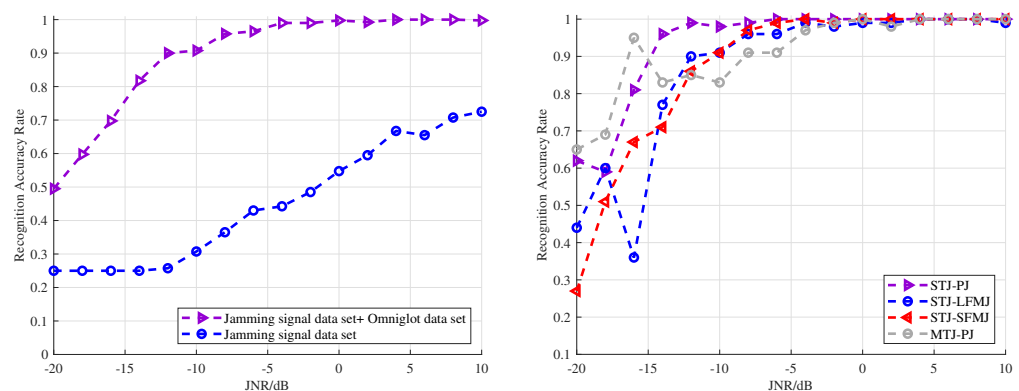


Figure 11. Recognition performance of MAML algorithm.

4.3. Multi-Node Collaborative Jamming Recognition Performance Based on MAML and Time–Frequency Analysis

In order to test the performance of the multi-node collaborative jamming recognition algorithm based on the time–frequency graph and MAML, we carried out a statistical experiment focusing on the accuracy of jamming recognition with different amounts of nodes. In order to ensure the accuracy of the experimental results, this article organized 100 Monte Carlo experiments under each JNR, and drew the comparison curve of recognition accuracy under different amounts of nodes.

As shown in Figure 12, one node has very poor identification performance. Especially at low JNR, the accuracy of jamming recognition results based on MAML and time–frequency graphs is obviously very low. For example, when $JNR = -18$ dB, the recognition accuracy was only 59.75%. With the increase in the amount of cognitive nodes, the accuracy of jamming recognition showed an increasing trend after the integration of the multi-node collaborative algorithm. When there were 21 cognitive nodes, the jamming recognition accuracy of $JNR = -18$ dB was improved to 73%, which is 13.25% higher than

that of a single node. This is because the jamming information observed by the multi-node cooperative system has diversity, that is, the same jamming signal will be observed by multiple nodes. This diversity can improve the reliability of the jamming recognition system, thereby reducing the global jamming recognition error caused by the single node identification error. At the same time, we discovered that with the number of nodes increased to 9, the improvement of jamming recognition accuracy will become limited by further increasing the number of cognitive nodes. By observing the confusion matrix, as shown in Figure 13, when $JNR = -18$ dB, the jamming recognition algorithm based on multi-node cooperation not only guaranteed the recognition accuracy of STJ-PJ and STJ-LFMJ, but also effectively improved the recognition accuracy of STJ-SFMJ and MTJ-PJ.

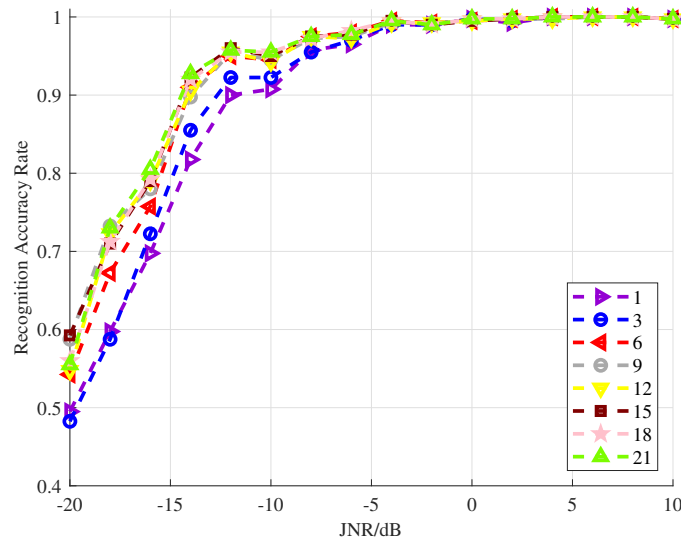


Figure 12. Multi-node collaborative compound jamming recognition based on MAML and time-frequency image.

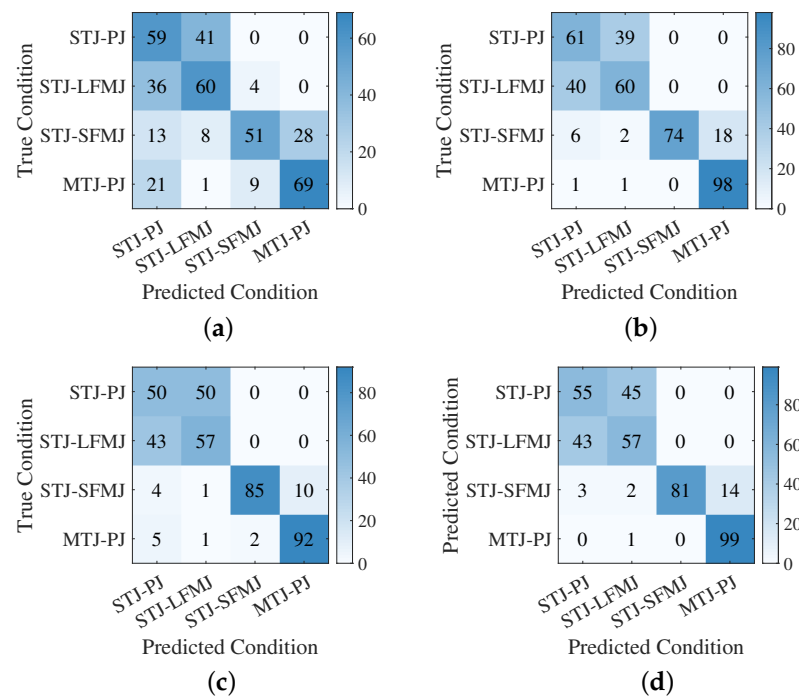


Figure 13. Confusion matrix with different amounts of nodes when $JNR = -18$ dB. (a) Confusion matrix with one node. (b) Confusion matrix under 9 nodes. (c) Confusion matrix under 15 nodes. (d) Confusion matrix under 21 nodes.

5. Conclusions

This article proposed a multi-node collaborative compound jamming recognition algorithm based on the time–frequency graph and MAML. In this article, the Omniglot dataset was used to extend the jamming signal dataset. The simulation results proved that this scheme can recognize compound jamming signals with very limited samples and still ensure high recognition accuracy. At the same time, the integration of the idea of multi-node collaboration can provide a variety of jamming observation information for the recognition system. The recognition system could effectively improve the recognition accuracy of compound jamming by synthesizing the observation results of multiple nodes.

6. Limits and Future Work

This article only studied the jamming recognition in the Gaussian channel. In a real-life environment, other more complex channel types might appear. Therefore, the research results might not be able to be used directly in more diverse communication environments. In addition, the mode decision fusion rule based on the multi-node collaborative compound jamming recognition algorithm proposed in this article is relatively simple. This rule directly assumes that each node contributes the same to the final decision result. However, in the real environment, each node might appear to have a different JNR. In this case, the node with higher JNR obviously needs to be assigned higher priority. Finally, in the process of recognition, the silent period is accepted by default. Only jamming and noise were considered. Yet, other communication signals could also exist in the real communication scene. These could be reserved for future study.

Author Contributions: Conceptualization, Q.Z. and S.H.; Methodology, Q.Z. and S.H.; Software, Q.Z., S.H. and W.C.; Validation, Q.Z. and W.C.; Formal Analysis, J.H.; Investigation, Q.Z. and S.H. and J.H.; Resources, Q.Z. and S.H.; Data Curation, Q.Z., S.H. and W.C.; Writing—Original Draft Preparation, S.H.; Writing—Review and Editing, S.H. and C.G.; Visualization, Q.Z., W.C. and J.H.; Supervision, C.G.; Project Administration, C.G. All authors have read and agreed to the published version of the manuscript.

Funding: This research received no external funding.

Data Availability Statement: Data are contained within the article.

Conflicts of Interest: Author Jing He was employed by the company Power China Sichuan Electronic Power Engineering Co., Ltd. The remaining authors declare that the research was conducted in the absence of any commercial or financial relationships that could be construed as a potential conflict of interest.

References

1. Säily, M.; Yılmaz, O.N.C.; Michalopoulos, D.S.; Pérez, E.; Keating, R.; Schaepperle, J. Positioning technology trends and solutions toward 6G. In Proceedings of the 2021 IEEE 32nd Annual International Symposium on Personal, Indoor and Mobile Radio Communications (PIMRC), Helsinki, Finland, 13–16 September 2021; pp. 1–7.
2. Wang, X.; Yang, J.; Huang, M.; Peng, Z. GNSS interference and spoofing dataset. *Data Brief* **2024**, *54*, 142–149. [[CrossRef](#)] [[PubMed](#)]
3. Wang, X.; Xu, Y.; Chen, J.; Li, C.; Liu, X.; Liu, D.; Xu, Y. Mean field reinforcement learning based anti-jamming communications for ultra-dense internet of things in 6G. In Proceedings of the 2020 International Conference on Wireless Communications and Signal Processing (WCSP), Nanjing, China, 21–23 October 2020; pp. 195–200.
4. Wang, Z.; Liu, R.; Liu, Q.; Han, L.; Thompson, J.S. Feasibility study of UAV-assisted anti-jamming positioning. *IEEE Trans. Veh. Technol.* **2021**, *70*, 7718–7733. [[CrossRef](#)]
5. Kong, Y.; Xia, S.; Dong, L.; Yu, X.; Cui, G. Compound Jamming Recognition via Contrastive Learning for Distributed MIMO Radars. *IEEE Trans. Veh. Technol.* **2024**, *73*, 7892–7907. [[CrossRef](#)]
6. Qin, J.; Zhang, F.; Wang, K.; Zuo, Y.; Deng, C. Interference signal feature extraction and pattern classification algorithm based on deep learning. *Electronics* **2022**, *11*, 2251. [[CrossRef](#)]
7. Zhanlin, H.; Jingning, W.; Chen, Z. A new multi-node cooperative interference detection and recognition algorithm based on SVM. In Proceedings of the 2014 International Conference on Information and Communications Technologies (ICT 2014), Nanjing, China, 15–17 May 2014; pp. 1–5.
8. Shu, J.; Liao, Y.; Luan, X. An Interference Recognition Method Based on Improved Genetic Algorithm. In Proceedings of the 2021 7th International Conference on Computer and Communications (ICCC), Chengdu, China, 10–13 December 2021; pp. 496–500.

9. Xu, J.; Ying, S.; Li, H. GPS interference signal recognition based on machine learning. *Mob. Netw. Appl.* **2020**, *25*, 2336–2350. [[CrossRef](#)]
10. Duan, C.; Feng, S.; Hu, H.; Luo, Z. A one-dimension convolutional neural network based interference classification method. *Phys. Commun.* **2023**, *59*, 102075–102083. [[CrossRef](#)]
11. Kulin, M.; Kazaz, T.; Moerman, I.; De Poorter, E. A deep learning approach for wireless signal identification in spectrum monitoring applications. *IEEE Access* **2018**, *6*, 18484–18501. [[CrossRef](#)]
12. Wang, P.; Cheng, Y.; Dong, B.; Peng, Q.; Li, S. Multi-Domain Networks for Wireless Recognition. *IEEE Trans. Veh. Technol.* **2022**, *71*, 6534–6547. [[CrossRef](#)]
13. Li, M.; Ren, Q.; Wu, J. Interference classification and identification of TDCS based on improved convolutional neural network. *J. Phys. Conf. Ser.* **2020**, *1651*, 012155. [[CrossRef](#)]
14. Swinney C.J.; Woods, J.C. The effect of real-world interference on CNN feature extraction and machine learning classification of unmanned aerial systems. *Aerospace* **2021**, *8*, 179. [[CrossRef](#)]
15. Durak, L.; Arikan, O. Short-Time Fourier Transform: Two fundamental properties and an optimal implementation. *IEEE Trans. Signal Process.* **2003**, *51*, 1231–1242. [[CrossRef](#)]
16. Jeon, H.; Jung, Y.; Lee, S.; Jung, Y. Area-efficient short-time fourier transform processor for time–frequency analysis of non-stationary signals. *Appl. Sci.* **2020**, *10*, 7208. [[CrossRef](#)]
17. Zhang, C.; Cui, Q.; Ren, S. Few-shot medical image classification with MAML based on dice loss. In Proceedings of the 2022 IEEE 2nd International Conference on Data Science and Computer Application (ICDSCA), Dalian, China, 28–30 October 2022; pp. 348–351.
18. Fu, S.; Cheng, N.; Zhang, N.; Jian, X.; Lyu, F.; Wen, H.; Shen, X.S. Virtualization enabled multi-point cooperation with convergence of communication, caching, and computing. *IEEE Netw.* **2020**, *34*, 94–100. [[CrossRef](#)]
19. Chen, M.; Zheng, W.; Vijayakumar, P.; Alazab, M.; Sivaraman, A. A multi-node collaborative decision-making scheme for privacy protection in IIoT. *IEEE Trans. Ind. Inform.* **2023**, *19*, 11531–11541. [[CrossRef](#)]
20. Fu, S.; Gao, J.; Zhao, L. Collaborative multi-resource allocation in terrestrial-satellite network towards 6G. *IEEE Trans. Wirel. Commun.* **2021**, *20*, 7057–7071. [[CrossRef](#)]
21. Lake, B.M.; Salakhutdinov, R.; Tenenbaum, J.B. Human-level concept learning through probabilistic program induction. *Science* **2015**, *350*, 1332–1338. [[CrossRef](#)] [[PubMed](#)]

Disclaimer/Publisher’s Note: The statements, opinions and data contained in all publications are solely those of the individual author(s) and contributor(s) and not of MDPI and/or the editor(s). MDPI and/or the editor(s) disclaim responsibility for any injury to people or property resulting from any ideas, methods, instructions or products referred to in the content.